Published in final edited form as:
Magn Reson Med. 2009 May ; 61(5): 1059–1065. doi:10.1002/mrm.21939.

Monitoring of Release of Cargo from Nanocarriers by MRI/MRS: Significance of T_2/T_2* Effect of Iron Particles

Yoshinori Kato and **Dmitri Artemov**
JHU ICMIC Program, The Russell H. Morgan Department of Radiology and Radiological Science, Johns Hopkins University School of Medicine, Baltimore, Maryland, U.S.A.

Abstract

To monitor the release of cargo molecules from nanocarriers, a novel MRI/MRS technique is developed and tested here. This novel approach uses a simultaneous encapsulation of superparamagnetic iron oxide (SPIO) nanoparticles and either a Gd-based paramagnetic contrast agent, GdDTPA-BMA, for MRI, or an anticancer agent, 5-fluorouracil (5-FU), for MRS. These agents have significantly different diffusion properties due to their different molecular sizes. Strong negative signal enhancement due to the T_2 effects of SPIO dominates the positive T_1 contrast generated by GdDTPA-BMA when SPIO and GdDTPA-BMA are in close proximity (intact form). Positive T_1 contrast becomes evident upon release of GdDTPA-BMA from the carrier once the distance between GdDTPA-BMA and SPIO molecules is beyond the T_2 enhancement range. Similarly, intact nanocarriers loaded with 5-FU and SPIO have a broad ^{19}F resonance line because line-width is inversely proportional to T_2*, while free 5-FU appears as a narrow resonance line once it is released from the liposomes. This technique allowed monitoring of the release of cargo molecules from liposomes encapsulating both SPIO and either GdDTPA-BMA or 5-FU by MRI/MRS *in vitro* using 2% agarose gel phantoms. Experimental results demonstrate successful demarcation of the released cargo molecules *vs*. encapsulated molecules.

Keywords

MRI; MRS; Dual contrast technique; Fe-based contrast agents; Gd-based contrast agents; 5-Fluorouracil; Activated MR contrast agent

---

Nanocarriers play a significant role in targeted cancer chemotherapy both pre-clinically and clinically. Drug release is one of the key factors that determine the success of targeted cancer chemotherapy because undesirable bursts of drug release in the systemic circulation cause adverse effects, while incomplete drug release reduces the efficacy of encapsulated drugs. The noninvasive monitoring of drug release from nanocarriers is an ideal way to assess *in vivo* release characteristics. To date, no *in vivo* noninvasive imaging techniques have been developed to visualize the release of cargo molecules from nanocarriers. As cancer therapy typically requires long-term and repeated treatment protocols, nuclear imaging is not suitable to monitor the release in this situation. Activated optical imaging probes have been developed, but, as yet, these agents are not feasible in clinical settings due to low spatial resolution and depth penetration limits. Magnetic resonance imaging (MRI) is one imaging modality that is

*Corresponding author: Yoshinori Kato, Ph.D., Phone: +1-410-502-5645, FAX: +1-410-614-1948, E-mail: E-mail: ykato@mri.jhu.edu, Dmitri Artemov, Ph.D., Phone: +1-410-614-2703, FAX: +1-410-614-1948, E-mail: dmitri@mri.jhu.edu, Address: Johns Hopkins University School of Medicine, Dept. of Radiology, 720 Rutland Ave., Traylor Bldg. #217, Baltimore, MD 21205, U.S.A.
Note: Y. Kato and D. Artemov contributed equally to the manuscript.

clinically feasible for longitudinal monitoring. Here, we demonstrate that MR can also be used to monitor the release of encapsulated compounds from carriers.

Two complementary approaches to visualize the release of encapsulated cargo from liposomal carriers were studied. In the first approach, MR imaging of two contrast agents coencapsulated in the liposome was used to monitor the release. In this experiment, a low molecular weight GdDTPA contrast agent was used as a surrogate imaging probe for encapsulated therapeutic compounds. In the second approach, direct MR spectroscopy of the encapsulated compound was used to monitor the release.

Clinical applications for contrast-enhanced MRI include diagnostic and functional imaging of diseased tissue. Gadolinium (Gd)-based contrast agents (such as GdDTPA) are representative of positive contrast agents, while superparamagnetic iron oxide (SPIO) nanoparticles are categorized as negative contrast agents. Both types of agents have been used extensively as a single agent, and concomitant use has also been attempted pre-clinically (1) and clinically (2) to improve the contrast in diagnostic MR images. In this study, a novel strategy for MRI/MR spectroscopy (MRS) has been developed to visualize the release of cargo molecules from nanocarriers by encapsulating both a negative contrast agent and either a positive contrast agent or an anticancer drug within a single carrier. This is the first technical report about monitoring the release of cargos using the dual-contrast technique.

For direct monitoring of cargo release from liposomal carriers, an MR-detectable anticancer drug, 5-Fluorouracil (5-FU), was used. 5-FU is a broad-spectrum antimetabolic agent that plays an important role in combination chemotherapeutic regimens for many types of cancer. As 5-FU has a fluorine atom that is detectable by ^{19}F MRS, *in vivo* MRS of 5-FU has been explored (3–6). ^{19}F is a preferred nucleus for *in vivo* MRS due to: i) high NMR sensitivity, second only to hydrogen; ii) lack of background from endogenous compounds; iii) intense NMR signals with a wide chemical shift range; and iv) availability of many fluorinated drugs for clinical use.

Therefore, to achieve the main goal of this study, the development of a noninvasive MR-based method to detect the release of cargo molecules, we have prepared and characterized liposomes encapsulating both SPIO and either gadolinium diethylenetriamine pentaacetic acid bismethylamide (GdDTPA-BMA) or 5-FU. We hypothesize that intact liposome generates strong negative signal enhancement due to the dominant T_2/T_2^* effects of SPIO over T_1 effect of GdDTPA-BMA in MRI and provides a broad resonance line of 5-FU due to the T_2^* effect of SPIO in MRS. Upon the release of GdDTPA-BMA and/or 5-FU from the liposome and their diffusion beyond the range of T_2/T_2^* effects of a relatively immobile SPIO, positive T_1 contrast of GdDTPA-BMA and a narrow resonance line of 5-FU are apparent. To prove our hypothesis, we also have demonstrated the visualization of the release of GdDTPA-BMA and 5-FU from liposomes by MRI and ^{19}F MRS, respectively, in a model *in vitro* system.

MATERIALS AND METHODS

Chemicals

Omniscan® (GdDTPA-BMA) was obtained from GE Healthcare (Chalfont St. Giles, Buckinghamshire, U.K.). Feridex® (SPIO) was obtained from Bayer Healthcare Pharmaceuticals, AG (Leverkusen, Germany). Fluorouracil Injection (5-FU) was purchased from APP Pharmaceuticals, Inc. (Schaumburg, IL). Distearoyl phosphatidylcholine (DSPC; M.W. 790.15), distearoyl phosphatidylethanolamine methoxypolyethylene glycol conjugate (DSPE-PEG; M.W. 2748), cholesterol (Cho; M.W. 386.65), agarose (type XI), Triton® X-100, Sephadex® G-50, and Sepharose® CL-2B were purchased from Sigma-Aldrich Co. (St. Louis, MO, U.S.A.).

Preparations of Liposomes Encapsulating GdDTPA-BMA/SPIO (Lip-Gd/Fe) and 5-FU/SPIO (Lip-FU/Fe)

Liposomes were prepared by the sonication method, followed by the extrusion method. The composition of liposomes prepared in this study was as follows: liposome membrane, DSPC/DSPE-PEG/Cho = 6.3/0.7/5.2 (μmol); and encapsulation media, 200 mM SPIO suspension and either 50 mM GdDTPA-BMA or 50 mg/mL 5-FU. Extrusion was performed using polycarbonate membranes (Avestin Inc., Ottawa, Canada) with a 200 nm pore-size, followed by a 100 nm pore-size (7,8). To remove unencapsulated SPIO particles (about 50 nm diameter) from 100–150 nm liposomes, the preparation was initially centrifuged at 500×*g* for 30 min twice and the supernatant was collected. Further, the liposomes were purified using a Sepharose® CL-2B column (H: 11.5 cm × d: 1.5 cm) with diluted PBS as the mobile phase. Free GdDTPA-BMA and 5-FU were removed by running the sample through a Sepharose® CL-2B column. Either way, 1 mL of the liposome fraction was collected. As controls, liposomes encapsulating either GdDTPA-BMA alone (Lip-Gd), 5-FU alone (Lip-FU), or SPIO alone (Lip-Fe) were also prepared.

In Vitro Characteristics of Liposomes

To determine particle size, size distribution, and ζ-potential of the resultant liposomes, dynamic laser-light scattering (DLS) measurements were performed using a Zetasizer Nano-ZS90 (Malvern Instruments Ltd., Worcestershire, U.K.).

GdDTPA-BMA contents in the collected 1 mL liposome fraction were determined by T_1 relaxation time measurement using MRI, after destruction of liposomes. Briefly, 500 μL of 10% Triton® X-100 solution was added to an equivalent volume of liposome suspension, and incubated at 70°C for 10 min to destroy liposomes. The mixture was centrifuged at 16,000×*g*, for 1 hr, to remove iron particles for Lip-Gd/Fe. T_1 relaxation time of the sample solution was measured with a Bruker Biospec 9.4T horizontal bore spectrometer (Bruker Biospin GmbH, Rheinstetten, Germany). Two hundred microliter of sample solution in a micro-centrifuge PCR tube was placed in the magnet. The same volumes of 5% Triton® X-100 solution and GdDTPA-BMA at different concentrations were used as standards. A saturation recovery snapshot-FLASH pulse sequence with an excitation pulse flip angle of 10 degrees, an echo time of 1.245 ms, and twelve T_1 saturation recovery delays (0.01, 0.05, 0.1, 0.2, 0.4, 0.6, 0.8, 1.2, 2.0, 3.0, 5.0, and 10.0 sec) were used (9). T_1 values of the samples were calculated using custom-written software in the IDL programming environment (ITT Visual Information Solutions Corp., Boulder, CO).

5-FU contents in a 1 mL liposome fraction were determined using high-performance liquid chromatography (HPLC), after destruction of liposomes in the same manner as described above. Briefly, 20 μL of the sample solution was directly injected into a Waters 1525 binary HPLC pump equipped with a Waters Symmetry® C_{18} reversed phase column (4.6 mm ϕ × 150 mm) and a Waters 2487 dual λ absorbance detector set at 266 nm. The mobile phase was comprised of a mixture of water and methanol (90:10, v/v), and the pH was adjusted to 3.2 with perchloric acid. The flow rate was 1.0 mL/min, and HPLC analysis was performed at room temperature. The Breeze 3.30 program (Waters Corp., Milford, MA) was used as acquisition and analysis software. 5-FU with five different known concentrations (50 ng/mL – 500 μg/mL) was used for a calibration curve.

The encapsulation of SPIO nanoparticles in liposomes was confirmed using atomic force microscopy (AFM). For AFM analysis, vesicles were deposited on mica wafers for 10 min, washed with water, and air-dried. All images were acquired in tapping mode immediately after preparation of the samples.

In Vitro Release Visualization by MRI

A total of 120 μL of 2%(w/v) agarose gel was cast in a micro-centrifuge PCR tube, and a mixture of 40 μL of liposome samples and 40 μL of either PBS (pH 7.4) or 10 mM Triton® X-100 were placed on the agarose gel layer. The same volume of Lip, Lip-Gd, and Lip-Fe were used as controls. Phantoms were imaged on a horizontal 9.4T MR scanner, using Paravision 3.0.2 software, at 1 and 6 hr following the addition of PBS or Triton® X-100. To position the PCR micro-centrifuge tubes with gel in the 10 mm RF coil (Bruker Biospin GmbH), a small plastic insert was used. A tripilot imaging sequence was used for reproducible positioning of the sample in the magnet at each MRI session. A multi-slice, multi-echo pulse sequence with an echo time of 15 ms, and six different repetition times (TR = 250, 500, 1,000, 2,000, 4,000, 8,000 ms), was used. To check the top-to-bottom T_1 changes in the agarose gel layer, three sagittal slices with 1 mm slice thickness were used. Quantitative T_1 maps of the samples were constructed using custom-written software in the IDL programming environment, and final analysis was performed with the ImageJ® program (National Institutes of Health, Bethesda, MD).

In Vitro Release Visualization by MRS

To detect drug release with MRS, phantom experiments were performed using a 2% agarose gel system in manner similar to that in the *in vitro* MRI study, as described above. MRS experiments were performed with a 9.4T MR scanner equipped with 121 mm-diameter shielded gradients and a $^{1}H/^{19}F$ RF coil, using Paravision 3.0.2 acquisition software. First, a Lip-FU/Fe suspension sample was placed in the magnet, and triplanar images were obtained to check the sample position, followed by multi-slice multi-echo sequences for a reference image. After manual shimming with ^{1}H channel, a ^{19}F spectrum was acquired. Then, 150 μL of 10% Triton® X-100 were added to the suspension in the upper compartment, followed by mild pipetting to disassemble liposomes, and ^{19}F MRS was acquired five hrs after the addition of Triton® X-100. Acquisition parameters for ^{19}F spectroscopy were as follows: number of acquisitions = 4096; number of points = 2048; sweep width = 10,000 Hz; repetition time = 1 sec; and flip angle = 90°.

RESULTS

Characterization of Liposomes

The hydrodynamic diameter of all liposome samples was consistently around 120–130 nm, and the ζ-potential was about −11 mV in all liposome samples, as summarized in Table 1. Liposomes contain about 0.35 and 1.5 μmol of GdDTPA-BMA and 5-FU, respectively, in each 1 mL fraction. AFM images obtained from the liposome preparation confirmed that one or two SPIO particles were typically encapsulated in a single liposome (Figure 1).

In Vitro Release Visualization

The release and distribution of GdDTPA-BMA from Lip-Gd/Fe were monitored using 2%(w/v) agarose gel phantom. As expected, intact SPIO-loaded liposomes (Lip-Gd/Fe and Lip-Fe) completely suppressed the MR signal of the suspension in the upper chamber of the platform due to significant shortening of T_2/T_2^* relaxation times, as shown in Figure 2. We also found that free GdDTPA-BMA diffused rapidly into a 2% agarose gel layer over time, while SPIO did not diffuse into the agarose matrix, even after six hrs, due to the larger size. GdDTPA-BMA release was more pronounced when liposomes were treated with detergent Triton® X-100 solution. It is worth noting that, in the case of Lip-Gd/Fe, GdDTPA-BMA molecules released from liposomes reduced the T_1 value dose-dependently of distance from the interface of the liposome suspension and agarose gel layer, once the molecules reached the areas beyond the diffusion range of SPIO, even though free SPIO particles also existed in the suspension.

In preliminary experiments to assess the diffusion of 5-FU into the agarose gel layer, the 5-FU solution (20 mg/mL) was placed on a 2% agarose gel, and removed after three hrs, and the gel surface was washed with PBS several times. The peak of 5-FU was easily detected with 64 acquisitions, indicating that 5-FU molecules freely diffused into the 2% agarose gel layer and provide sufficient sensitivity for MRS. As shown in Figure 3, intact liposomes loaded with SPIO and 5-FU did not show the peak of 5-FU due to the predominant line-broadening T_2* effect of SPIO particles. Upon the release of 5-FU and diffusion away from the disrupted liposomes, a sharp peak was detected in the ^{19}F MR spectrum of the sample.

DISCUSSION

The particular emphasis of this study was on the novel use of SPIO nanoparticles for the noninvasive monitoring of cargo release from nanocarriers. The strategy is based on the use of a dual MR contrast agent, which is defined as a combination of a positive and a negative contrast agent within the same carrier. Utilization of the dominant T_2/T_2* effects of SPIO, and diffusion differences between SPIO and GdDTPA-BMA or 5-FU, made release monitoring with MRI/MRS possible. Noninvasive release monitoring using a dual MR contrast technique can also track distribution of a Gd-based contrast agent released from nanocarriers, possibly *in vivo*. This would be particularly useful in tumor tissue where the vessels/matrix have a unique character that small molecules, in this case, GdDTPA-BMA, can easily leak from tumor capillary vessels and diffuse through the interstitium, whereas large particles/molecules, in this case, SPIO, mostly stay in the perivascular space (10). With regard to release monitoring, the advantage of MRS over MRI is the direct detection of cargo drug, in this case 5-FU albeit with lower sensitivity/spatial resolution; in other words, MRS does not require contrast agents as a surrogate marker. MRI contrast agents affect the relaxation properties of bulk water molecules, and can be categorized as positive or negative agents according to their effect on image intensity during the course of a standard MRI experiment. SPIO nanoparticles produce large distortions in the local magnetic field due to their extremely high magnetic moment generated by the iron-oxide core. Empirical observations indicate that a single SPIO induces local inhomogeneities detectable in gradient-echo T_2*-weighted MR images at a distance of at least 50 times its size (11). Spin-echo acquisition sequences completely refocus stationary inhomogeneities of the local magnetic field, and therefore, T_2 effects depend on the diffusion of water molecules during the evolution time (or echo time) of the imaging sequence. For a typical diffusion coefficient of the fast-diffusing extracellular water in breast tumors *in vivo* with a $D \cong 10^{-3}$ mm^2/sec (12), and an echo time (TE) of 30 ms, the average radius of the area with strong T_2 contrast generated by SPIO nanoparticles can be estimated as $R \cong (6DT)^{1/2} \approx 15$ μm, which is at least an order of magnitude smaller than the currently available spatial resolution of MRI *in vivo*.

The mechanism of visualization of cargo release involves the diffusion of a low molecular weight GdDTPA or 5-FU from the areas of negative signal enhancement generated by massive SPIO nanoparticles (evaluated above) upon decomposition of the carrier vesicle. Estimating the diffusion coefficient of GdDTPA in tissue from the water self-diffusion coefficient using the Stokes-Einstein relation, $D = k_BT/6\pi\eta R$, where k_B is the Boltzmann's constant, T is the absolute temperature, η is the viscosity of the medium, and R is the radius of the particle, we obtain $D_{GdDTPA} \cong 2.5 \times 10^{-5}$ mm^2/sec. The typical time required for a GdDTPA molecule to diffuse 100 μm in the tissue can be estimated as $t_{GdDTPA} \cong 60$ sec, which is well within a reasonable experimental time. The low molecular weight Gd-based MR contrast agent can also be used as a surrogate marker for other small molecular agents, assuming their diffusion rates are similar. Strong negative signal enhancement, due to the T_2/T_2* effects of iron oxide nanoparticles, dominates the positive T_1 contrast generated by a Gd-based contrast agent when these agents are in close proximity, such as within an intact nanocarrier encapsulating GdDTPA/SPIO. Positive T_1 contrast becomes evident upon release of a Gd-based contrast agent from the carrier, once the distance between Gd-based contrast agents and SPIO molecules

is beyond the T_2 enhancement range. This phenomenon is based on a significant restriction of the free diffusion of massive SPIO nanoparticles due to their large sizes (40–70 nm), which results in a significantly shorter diffusion range over the same experimental time. Similar to the dual-contrast technique described above, the principle of release monitoring of 5-FU by MRS is that intact liposomes encapsulating 5-FU have a broad resonance line by co-encapsulation with SPIO, since line-width is inversely proportional to T_2* (13). Free 5-FU, however, appears as a narrow resonance line, once released, because the T_2* effects of SPIO on free 5-FU diminishes in regions beyond the diffusion range of SPIO.

Our *in vitro* results and the principles of release monitoring of both GdDTPA-BMA and 5-FU by MRI/MRS are summarized in Table 2. The findings obtained here provide direct support for our hypotheses: i) the T_2 effects of SPIO particles dominated the positive T_1 contrast of GdDTPA-BMA, as long as liposomes were in an intact form, which produced strong negative signal enhancement, while positive T_1 contrast became evident upon release of GdDTPA-BMA from the liposomes because the T_2 effects of SPIO diminished in regions beyond the diffusion range of SPIO; and ii) intact 5-FU-loaded liposomes showed a broad resonance line by co-encapsulation with SPIO because line-width was inversely proportional to T_2*, while a narrow resonance line was apparent upon release of 5-FU from the liposome because the T_2* effects of SPIO diminished in regions beyond the diffusion range of SPIO.

Images acquired with AFM indicated that it was difficult to remove free SPIO nanoparticles from the liposomes using current technology, such as gel filtration and centrifugation, because SPIO nanoparticles also have nanometer-range sizes. Martina et al. used a Sephacryl® S1000 superfine microcolumn (H: 5.8 cm × d: 0.4 cm) for purification of liposomes from magnetic fluid (14), which seems to have produced better separation compared to our results. Their liposome size was about 200 nm, and the iron particle size contained in the ferrofluid was 16 nm, while our liposome size was about 130 nm, and we used clinically approved Feridex® SPIO nanoparticles with a diameter of 40–70 nm. Smaller differences between liposomes and free particles make it difficult to completely remove SPIO particles. Although ideally, it would be preferable to eliminate all non-encapsulated molecules, currently, the presence of unencapsulated nanoscale iron-oxide particles will not interfere with future *in vivo* MR measurements. This is because it is well-established that free SPIO nanoparticles, administered systemically, predominantly accumulate in the liver (>80%) and the spleen (≈6%) due to capture by the reticuloendothelial system (15), and, since Feridex® SPIO is an FDA-approved contrast agent, and toxicity and clearance issues are relatively well understood, trace amounts of free iron-oxide particles are not associated with toxic side effects (15). In addition, due to the short diffusion range of free SPIO, the SPIO particles will most probably be localized in the sites of liposome accumulation, while small cargo molecules will diffuse to tumor tissue and generate positive MR contrast enhancement or a narrow resonance line, as implied by the *in vitro* phantom studies. Inherent difficulty in discriminating cargo release is encountered when spatial separation between Feridex® and GdDTPA-BMA is insufficient.

Although these *in vitro* experiments support the concept behind our strategy for noninvasive monitoring of drug release, the *in vivo* application of this technique will be challenging. Practical limitations include: i) the concentration of cargo molecules in tumor; and ii) a tumor microenvironment that is different from an *in vitro* agarose gel system. Our preliminary experiments showed that the dual MR contrast technique could noninvasively monitor liposome delivery, and cargo release after i.v. administration of liposomes up to 48 hr post-contrast, but could not visualize intratumoral distribution due to insufficient concentration to visualize this distribution in the tumor using quantitative T_1 mapping. Intratumoral administration of liposomes, however, allowed visualization of intratumoral spatial distribution of the intact contrast agent on T_2-weighted images, as well as the release of gadolinium contrast agent using quantitative T_1 mapping due to a sufficient concentration of

GdDTPA-BMA in tumor (unpublished data). Similar to our *in vitro* experiments, *in vivo* MRS of 5-FU will most likely be limited to single-voxel detection due to the limited sensitivity of ^{19}F MRS; the intratumoral spatial distribution of 5-FU would be difficult to measure. With regard to molecular diffusion in the tumor, intratumoral delivery of larger molecules is restricted due to the short diffusion distance from the vascular surface, compared to smaller molecules, as reported by Dreher et al. (10). In addition to our observation, this report also supports our novel concept that diffusion differences between small cargo molecules and large Fe-based negative contrast agents can be utilized to monitor drug release using this technique. In fact, SPIO particles were retained in the capillary vessels or in the perivascular space, and were not diffused into the interstitium after intravenous administration of Lip-Gd/Fe (unpublished data), in accordance with the results observed in an *in vitro* agarose gel system.

Aside from the limitation of this technique for *in vivo* use, this technique is versatile enough to provide i) traditional diagnostic imaging (1,2), ii) MRI/MRS signal activation reported here, and iii) double labeling of biomolecules with MR contrast agents that is currently underway. Although we have demonstrated here only monitoring of GdDTPA and 5-FU from conventional liposomes, this technique can also be used for other nanocarriers, such as nanospheres, micelles, polymeric carriers, etc., as well as for specific release monitoring, such as conjugates of SPIO with GdDTPA via oligo peptide spacers and smart nanocarriers including pH- or thermo-responsive nanocarriers.

Our *in vitro* experiments confirmed that diffusion differences play an important role in the emergence of the MRI/MRS signal, and thus, can be used as a novel mechanism for noninvasive monitoring of drug release. Although the *in vivo* application of this technique still faces technological obstacles, this report is an important first step toward the noninvasive MRI monitoring of release of cargo molecules.

Previously proposed techniques for “activated” MR contrast agents were based on the modulation of T_1 or T_2 relaxivity following changes in the molecular structure of the agent (16–18). The major limitation of this approach is the low dynamic range of the effect and dependence on the concentration of the agent. The new technique described in this paper involves the emergence of the MRI/MRS signal, in the sense that the MR signal goes from “low/no” (negative T_2 enhancement with SPIO on MRI, or a broad ^{19}F resonance line of SPIO with the T_2* effect of SPIO for MRS) to “high” (positive T_1 enhancement by GdDTPA-BMA for MRI or narrow ^{19}F resonance line of 5-FU for MRS). By combining T_2- and T_1-weighted imaging or MR spectroscopy, it is possible to simultaneously detect the presence of the intact agent, characterized by a negative T_2/T_2* enhancement signature, and to monitor the release of the cargo molecules by positive T_1 enhancement or the appearance of a narrow resonance line in the MR spectrum.

CONCLUSION

In this study, we have explored a novel method of specific MRI/MRS signal emergence, using a combination of SPIO nanoparticles and GdDTPA-BMA or 5-FU, and have successfully demonstrated the application of this method to monitor release from liposomes *in vitro* in an agarose gel system with MRI and MRS. The technique reported here can be applied to other controlled-release carrier systems, including nanoparticles and polymeric nanocarriers, and thus, can be used for drug development in preclinical models, as well as clinical settings, to monitor the release characteristics and subsequent distribution of drug molecules in the tumor *in vivo*. This novel method of modulation of MRI/MRS signals can provide important new opportunities for preclinial and clinical molecular imaging using MRI/MRS.

ACKNOWLEDGMENT

The authors thank Dr. Jan H. Hoh for assistance with atomic force microscopy, and Ms. Mary McAllister for editing this manuscript. This work was supported by The Nagai Foundation, Tokyo, NIH R21 EB008162, and in part by NIH P50 CA103175 (JHU ICMIC Program).

REFERENCES

1. Weissleder R, Saini S, Stark DD, Wittenberg J, Ferrucci JT. Dual-contrast MR imaging of liver cancer in rats. AJR Am J Roentgenol 1988;150(3):561–566. [PubMed: 3257610]
2. Suto Y, Shimatani Y. Dual contrast magnetic resonance imaging with combined use of positive and negative contrast agent in human hepatocellular carcinoma. Br J Radiol 1995;68(806):116–120. [PubMed: 7735739]
3. Aboagye EO, Artemov D, Senter PD, Bhujwalla ZM. Intratumoral conversion of 5-fluorocytosine to 5-fluorouracil by monoclonal antibody-cytosine deaminase conjugates: noninvasive detection of prodrug activation by magnetic resonance spectroscopy and spectroscopic imaging. Cancer Res 1998;58(18):4075–4078. [PubMed: 9751613]
4. Guerquin-Kern JL, Volk A, Chenu E, Lougerstay-Madec R, Monneret C, Florent JC, Carrez D, Croisy A. Direct *in vivo* observation of 5-fluorouracil release from a prodrug in human tumors heterotransplanted in nude mice: a magnetic resonance study. NMR Biomed 2000;13(5):306–310. [PubMed: 10960921]
5. Stevens AN, Morris PG, Iles RA, Sheldon PW, Griffiths JR. 5-fluorouracil metabolism monitored *in vivo* by ^{19}F NMR. Br J Cancer 1984;50(1):113–117. [PubMed: 6743508]
6. Wolf W, Presant CA, Servis KL, el-Tahtawy A, Albright MJ, Barker PB, Ring R 3rd, Atkinson D, Ong R, King M, Singh M, Ray M, Wiseman C, Blayney D, Shani J. Tumor trapping of 5-fluorouracil: *in vivo*^{19}F NMR spectroscopic pharmacokinetics in tumor-bearing humans and rabbits. Proc Natl Acad Sci U S A 1990;87(1):492–496. [PubMed: 2296605]
7. Olson F, Hunt CA, Szoka FC, Vail WJ, Papahadjopoulos D. Preparation of liposomes of defined size distribution by extrusion through polycarbonate membranes. Biochim Biophys Acta 1979;557(1):9–23. [PubMed: 95096]
8. MacDonald RC, MacDonald RI, Menco BPM, Takeshita K, Subbarao NKLH. Small-volume extrusion apparatus for preparing of large, unilamellar vesicles. Biochim Biophys Acta 1991;1061:297–303. [PubMed: 1998698]
9. Bhujwalla ZM, Artemov D, Natarajan K, Ackerstaff E, Solaiyappan M. Vascular differences detected by MRI for metastatic versus nonmetastatic breast and prostate cancer xenografts. Neoplasia 2001;3(2):143–153. [PubMed: 11420750]
10. Dreher MR, Liu W, Michelich CR, Dewhirst MW, Yuan F, Chilkoti A. Tumor vascular permeability, accumulation, and penetration of macromolecular drug carriers. J Natl Cancer Inst 2006;98(5):335–344. [PubMed: 16507830]
11. Shapiro EM, Skrtic S, Sharer K, Hill JM, Dunbar CE, Koretsky AP. MRI detection of single particles for cellular imaging. Proc Natl Acad Sci U S A 2004;101(30):10901–10906. [PubMed: 15256592]
12. Paran Y, Bendel P, Margalit R, Degani H. Water diffusion in the different microenvironments of breast cancer. NMR Biomed 2004;17(4):170–180. [PubMed: 15229930]
13. Walstedt RE, Walker LR. Nuclear-resonance line shapes due to magnetic impurities in metals. Phys Rev B 1974;9(11):4857–4867.
14. Martina MS, Fortin JP, Ménager C, Clément O, Barratt G, Grabielle-Madelmont C, Gazeau F, Cabuil V, Lesieur S. Generation of superparamagnetic liposomes revealed as highly efficient MRI contrast agents for *in vivo* imaging. J Am Chem Soc 2005;127(30):10676–10685. [PubMed: 16045355]
15. Weissleder R, Stark DD, Engelstad BL, Bacon BR, Compton CC, White DL, Jacobs P, Lewis J. Superparamagnetic iron oxide: pharmacokinetics and toxicity. AJR Am J Roentgenol 1989;152(1):167–173. [PubMed: 2783272]
16. Louie AY, Huber MM, Ahrens ET, Rothbacher U, Moats R, Jacobs RE, Fraser SE, Meade TJ. In vivo visualization of gene expression using magnetic resonance imaging. Nat Biotechnol 2000;18(3):321–325. [PubMed: 10700150]

17. Perez JM, Josephson L, O'Loughlin T, Hogemann D, Weissleder R. Magnetic relaxation switches capable of sensing molecular interactions. Nat Biotechnol 2002;20(8):816–820. [PubMed: 12134166]

18. Zhao M, Josephson L, Tang Y, Weissleder R. Magnetic sensors for protease assays. Angew Chem Int Ed Engl 2003;42(12):1375–1378. [PubMed: 12671972]

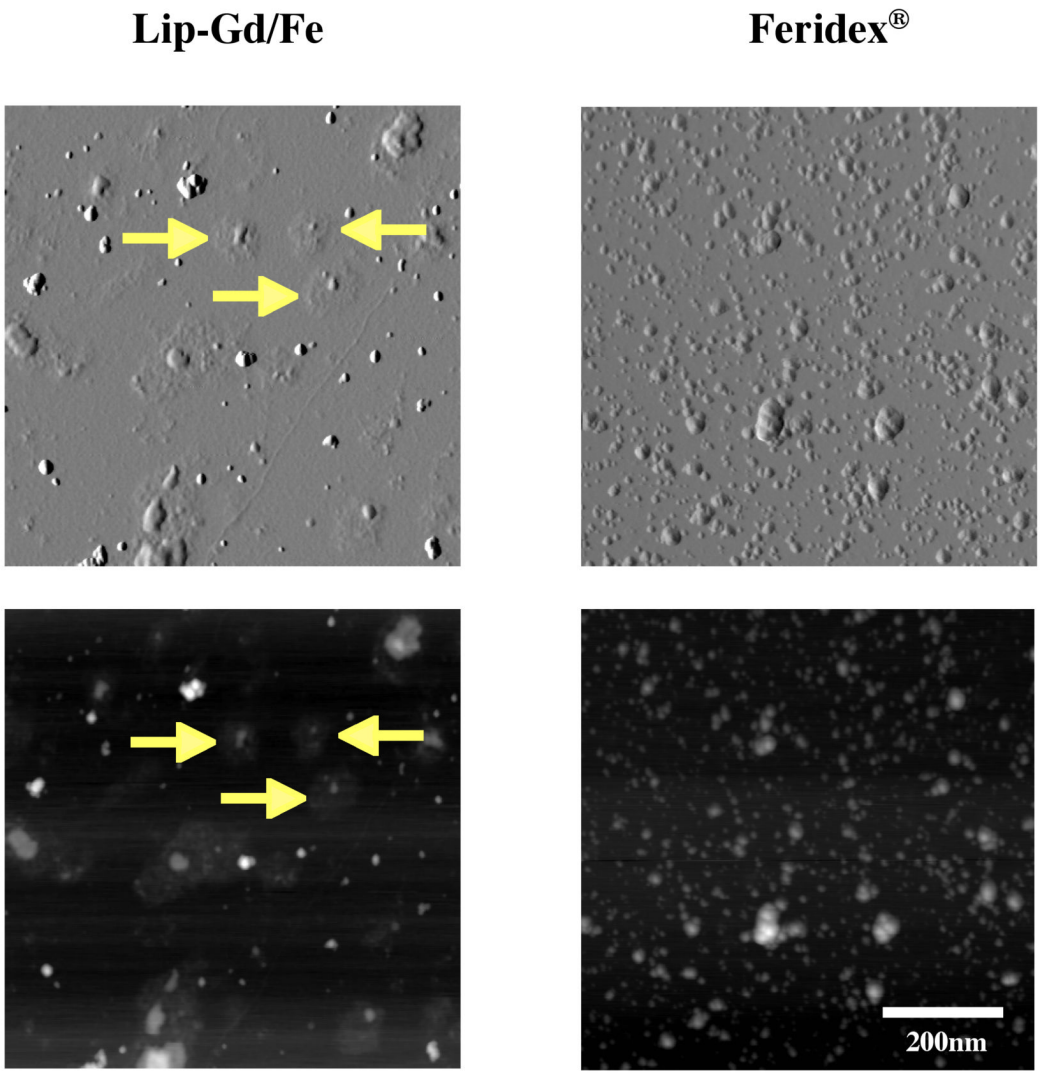

FIG. 1.

AFM images of liposomes encapsulating a mixture of GdDTPA-BMA and SPIO nanoparticles (left panel). For comparison, Feridex® SPIO medium alone was imaged, and is shown in the right panel. AFM images on the top show 3D level plots, and bottom panels show the same images in the brightness-modulated mode. Arrows in the figure indicate the positions of encapsulated SPIO in liposomes, visible as elevated knobs surrounded by remnants of the liposomal lipid bilayer. Images were acquired with 512×512 points and 2 nm in-plane resolution. GdDTPA-BMA molecules were not visible in the images due to their small molecular size.

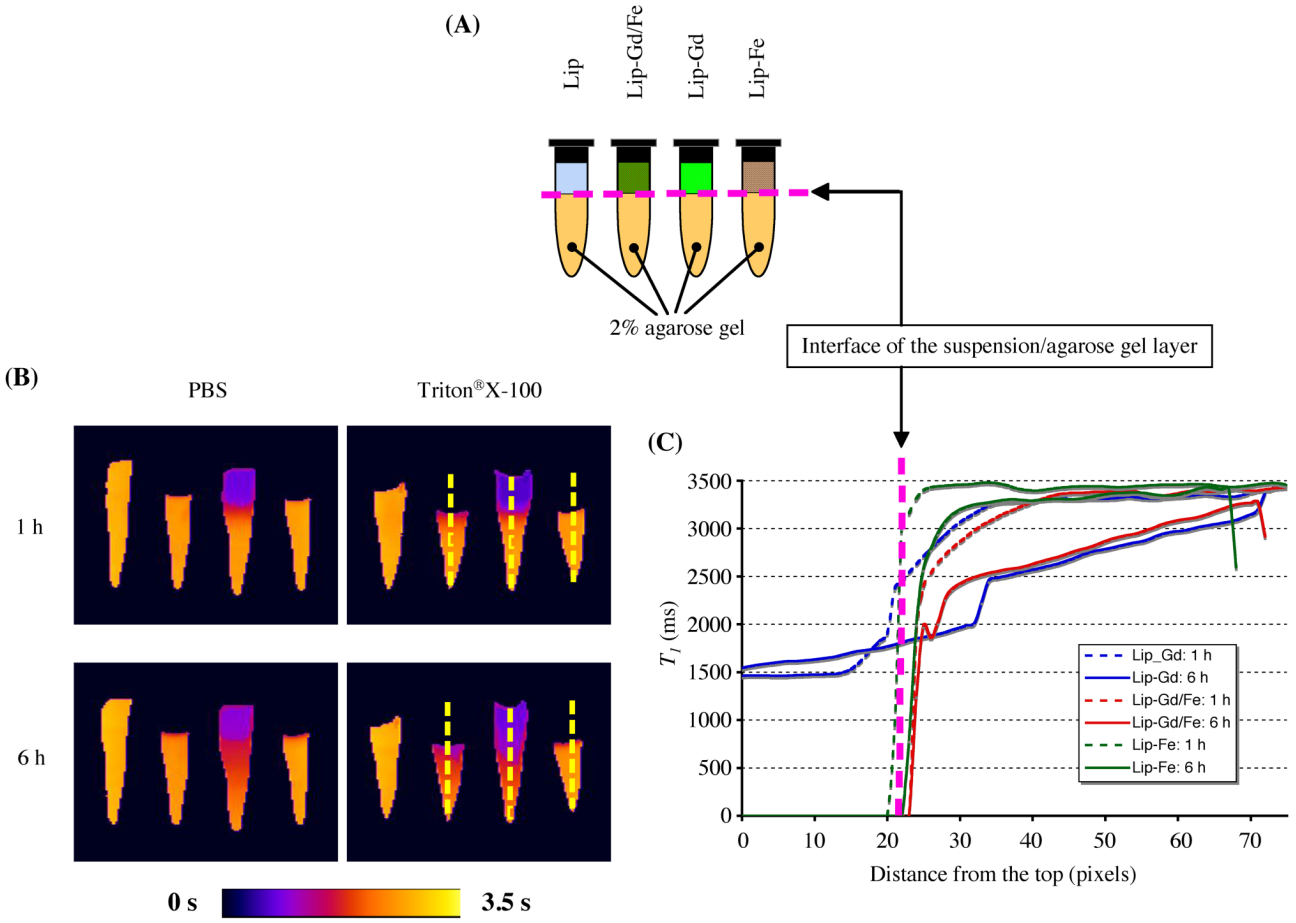

FIG. 2.

Visualization of the *in vitro* release of Gd-based contrast agent by the dual MR contrast agent technique. **(A)** Schematic of liposome phantoms. A mixture of 40 μL of liposome samples and 40 μL of either PBS (pH 7.4) or 10 mM Triton® X-100 were placed on the 2% agarose gel layer. **(B)** Quantitative T_1 maps of liposome phantoms. Parameters for MRI are as follows: field of view = 40 × 22 mm; matrix size = 128 × 80; echo time = 15 ms; number of acquisitions = 2; three sagittal slices (slice thickness = 1 mm). **(C)** Diffusion profiles are expressed as a T_1 value as a function of distance from the interface. Diffusion profiles of Lip-Gd/Fe in a 2% agarose gel layer were comparable to that of the free Gd-based contrast agent released from Lip-Gd.

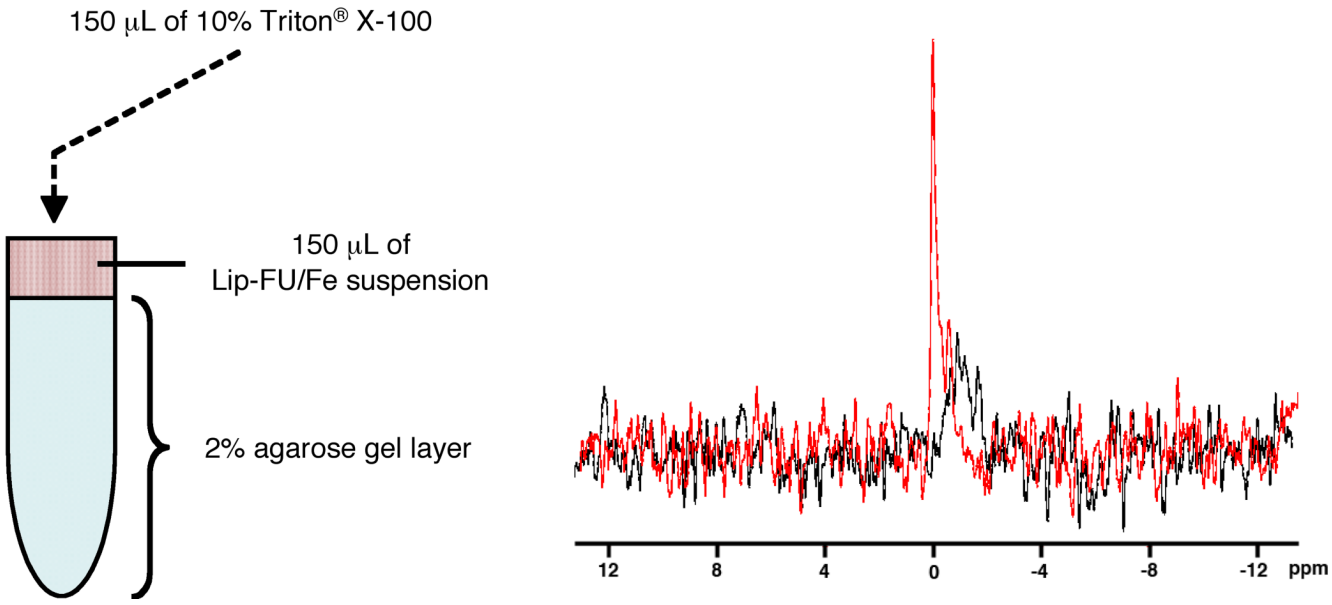

FIG. 3.

In vitro detection of 5-FU release from liposome suspension (Lip-FU/Fe) using ^{19}F MRS. **(A)** Schematic of liposome phantoms. **(B)** ^{19}F Spectra of Lip-FU/Fe suspension on a 2% agarose gel, pre- and post-Triton® X-100 treatment. The same acquisition parameters were used for both samples. Black spectrum: pre-treatment; Red spectrum: post-Triton® X-100 treatment. Each acquisition required about 68 min.

Table 1

In vitro characteristics of liposomes collected using Sepharose® CL-2B gel column

	Diameter (nm) *1, *2		Polydispersity Index ± S.D.	ζ-potential (mV) ± ζ deviation *1	Gd or FU amount (μmol) ± S.D. *3
	Mode ± S.D.	Mean ± width			
Lip	118 ± 21	127 ± 28	0.09 ± 0.08	−11 ± 7	—
Lip-Gd	117 ± 9	125 ± 26	0.03 ± 0.02	−9 ± 8	0.34 ± 0.02
Lip-FU	111 ± 9	123 ± 27	0.03 ± 0.02	−11 ± 8	1.30 ± 0.09
Lip-Fe	129 ± 6	139 ± 27	0.04 ± 0.03	−11 ± 8	—
Lip-Gd/Fe	125 ± 6	138 ± 33	0.11 ± 0.06	−11 ± 7	0.38 ± 0.10
Lip-FU/Fe	129 ± 12	141 ± 32	0.04 ± 0.02	−12 ± 8	1.73 ± 0.31

*1 Liposomes were dispersed in PBS (pH 7.4) for the size measurement, and dispersed in 10 mM of NaCl for the ζ-potential measurement.

*2 The hydrodynamic diameter of liposomes was calculated by the Stokes-Einstein equation.

*3 Amount of GdDTPA-BMA or 5-FU in 1 mL liposome fraction collected using Sepharose® CL-2B gel column.

Table 2

Principle of release monitoring of cargo molecules by MRI/MRS

	Molecular weight / size	Diffusion	MRI signal enhancement	MRS peak
Intact liposome	≈ 120 nm	±	– *1	***Broad*** *2
Released GdDTPA-BMA	≈ 591 Da	+++	+++	N/A
Released 5-FU	130 Da	+++	N/A	***Narrow***
SPIO nanoparticle	40–70 nm	±	– *1	N/A *2

*1 T_2 effect of SPIO particles dominates the positive T_1 contrast of GdDTPA, thus intact forms generate strong negative signal enhancement.

2 T_2 effect of SPIO broadens 5-FU peak, thus intact forms generate a broad resonance line.